1

Adaptive Unscented Kalman Filter and Its Applications in Nonlinear Control

Jianda Han, Qi Song and Yuqing He
State Key Laboratory of Robotics
Shenyang Institute of Automation
Chinese Academy of Sciences
P.R.China

1. Introduction

Active estimation is becoming a more important issue in control theory and its application, especially in the nonlinear control of uncertain systems, such as robots and unmanned vehicles where time-varying parameters and uncertainties exist extensively in the dynamics and working environment.

Among the available techniques for active modeling, Neural Networks (NN) and NN-based self learning have been proposed as one of the most effective approaches in 1990s (Pesonen et al., 2004). However the problems involved in NN, such as training data selection, online guaranteed convergence, robustness, reliability and real-time implementation, still remain open and limit its application in real systems, especially those requiring high reliable control.

Most recently, the encouraging achievements in sequential estimation makes it becoming an important direction for online modeling and model-reference control (Napolitano, et al., 2000). Among stochastic estimations, the most popular one for nonlinear system is the Extended Kalman Filter (EKF). Although widely used, EKF suffers from the deficiencies including the requirement of sufficient differentiability of the state dynamics, the susceptibility to bias and divergence during the estimation. Unscented Kalman Filter (UKF) (Julier et al., 1995; Wan & Van der Merwe, 2000) provides a derivative-free way to the state parameter estimation of nonlinear systems by introducing the so called 'unscented transformation', while achieving the second-order accuracy (the accuracy of EKF is first order) with the same computational complexity as that of EKF.

Although the nonlinear state dynamics are used without linearization and the calculations on Jacobians or Hessians are not involved, UKF still falls into the framework of Kalman-type filters, which can only achieve good performance under *a priori* assumptions (Jazwinski, 1970), which includes: 1) accurate reference models, 2) complete information of the noise distribution, and 3) proper initial conditions. However, such *a priori* knowledge is often not accurate, or even not available in practice. The normal UKF will suffer from performance degradation or even instability due to the mismatch between the *a priori* assumptions and the real ones within the system to be controlled.

One of the approaches solving this problem is to introduce adaptive mechanism into a normal filter, i.e., the adaptive law automatically tunes the filter parameters to match the

Open Access Database www.intechweb.org

Source: Kalman Filter: Recent Advances and Applications, Book edited by: Victor M. Moreno and Alberto Pigazo,
ISBN 978-953-307-000-1, pp. 584, April 2009, I-Tech, Vienna, Austria

real statistics that are insufficiently known as *a priori*. During the past decade, there have been some investigations in the area of adaptive filter, and most of them are constructed with respect to the KF or EKF. Mohamed et al. (Mohamed et al., 1999) studied the performance of multiple-model-based adaptive Kalman Filter for vehicle navigation using GPS. Loebis et al. (Loebis et al., 2004) proposed an adaptive EKF algorithm, which adjusted the measurement noise covariance matrix by fuzzy logic. Other works can also be seen in references (Noriega & Pasupathy, 1997; Mehra, 1970; Hu et al., 2003; Chaer et al., 1997; Garcia-Velo, 1997). As far as the adaptive UKF (AUKF) is concerned, the most-often-mentioned scheme was proposed by Lee and Alfriend (Lee & Alfriend, 2004), where the Maybeck's method (Maybeck, 1979) was modified by maximum-likelihood principle to estimate the error covariance matrix, and this estimator was further integrated into the normal UKF as the adaptive mechanism.

In this Chapter, we first introduce the normal UKF algorithm. Then, two adaptive UKFs, which are the MIT-rule-based AUKF (MIT-AUKF) and master-slave AUKF (MS-AUKF), are proposed and analyzed in detail. In the MIT-AUKF: a cost function is first constructed from the error between the covariance matrix of innovation and their corresponding estimations; then, an MIT-like adaptive law is designed to online update the covariance of the process noise with the purpose of minimizing the cost function; and finally, the updated covariance is fed back into the normal UKF to realize the adaptive performance. The MS-AUKF, on the other hand, is composed of two parallel UKFs, where the master UKF is used to estimate the states or parameters as a normal UKF, and the slave one is dedicated to estimating the noise covariance matrix for the master UKF.

In order to demonstrate their applications, the proposed AUKFs are tested with respect to the dynamics of an omni-directional mobile robot and a model unmanned helicopter. The improvements achieved from the adaptive mechanisms are demonstrated by the comparisons between the simulation results of the AUKFs and those of the normal UKF. Moreover, the integration of AUKF into robust control scheme is also introduced in the end.

The Chapter is organized as follows: the unscented transformation (UT) and normal UKF are introduced in Section II. The MIT-AUKF and MS-AUKF are described in Section III and IV respectively. Simulations on both UKF and AUKF with respect to the joint estimation of states and parameters, as well as the integration of AUKF into robust control, are provided in Section V, followed by the conclusions.

2. UT and normal UKF

Instead of propagating the Gaussian variables through the first-order linearization model as EKF does, UKF uses the Unscented Transformation (UT) to handle the nonlinear plant directly. UT provides an approach to approximate the statistics of a nonlinear transformation like Eq. (1) by a finite set of 'sigma points'.

$$\kappa = g(\delta) \tag{1}$$

where $g(\cdot)$ is a nonlinear function, and δ denotes an $n\times1$ stochastic variable with the mean of $\bar{\delta}$ and the covariance of P_δ.

In order to calculate the propagation statistics of δ through $g(\cdot)$, i.e., the mean (κ) and covariance (P_κ) of the output κ, the UT uses the following steps (see Fig. 1 also).

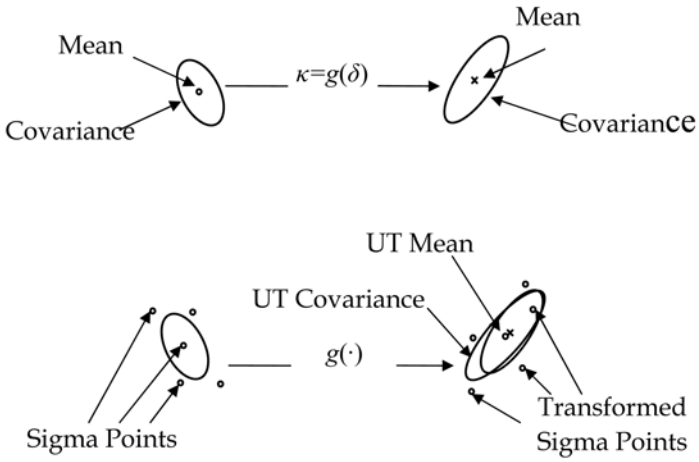

Fig. 1. Unscented Transformation

***UT-I:* Definition of Sigma Points**

The distribution of κ can be approximated by a finite set of sigma points. These sigma points are calculated from the *a priori* mean and covariance of δ by the following equations,

$$\begin{cases} \chi_0 = \bar{\delta} \\ \chi_i = \bar{\delta} + (\sqrt{(L+\lambda)P_\delta})_{i,:} & i = 1,\cdots,L \\ \chi_i = \bar{\delta} - (\sqrt{(L+\lambda)P_\delta})_{i-L,:} & i = L+1,\cdots,2L \end{cases} \tag{2}$$

$$\lambda = L(\alpha^2 - 1) \tag{3}$$

where $(\cdot)_i$ denotes the ith row of matrix $(\cdot)$, L is the number of sigma point, α and λ are both constants, and α determines the spread of the sigma points.

***UT-II:* Propagating of Sigma Points**

Computing the transformation from the input δ-space to the output κ-space of each sigma point by Eq. (1), i.e.,

$$\gamma_i = g(\chi_i) \qquad i = 1,\cdots,2L \tag{4}$$

***UT-III:* Calculating the Mean and Covariance of output κ**

$$\begin{cases} \bar{\kappa} = \sum_{i=0}^{2L} w_i^m \gamma_i \\ P_\kappa = \sum_{i=0}^{2L} w_i^c (\gamma_i - \bar{\kappa})(\gamma_i - \bar{\kappa})^T \end{cases} \tag{5}$$

where the weights of w_i^m and w_i^c are calculated by

$$\begin{cases} w_0^m = \dfrac{\lambda}{L+\lambda} \\ w_0^c = \dfrac{\lambda}{L+\lambda} + (1-\alpha^2+\beta) \\ w_i^m = w_i^c = \dfrac{1}{2(L+\lambda)} \qquad i = 1,\cdots,2L \end{cases} \tag{6}$$

and β is a constant with the purpose of incorporating part of the prior knowledge of the distribution of δ. It has been proved that, for Gaussian distributions, $\beta = 2$ is optimal (Van der Merwe & Wan, 2001).
With respect to the control application of a nonlinear system of Eq. (7),

$$\begin{cases} x_{k+1} = f(x_k) + w_k \\ y_k = h(x_k) + v_k \end{cases} \tag{7}$$

where $x_k \in R^n$, and $y_k \in R^m$ are respectively, the state and output vector at time k; w_k and v_k are the process and measurement noise vector, which are both assumed to be Gaussian white noise with zero mean and covariance R_w and R_v; the normal UKF can be deduced as followings.
UKF-I: **Initialization**

$$\begin{cases} x_0 = E[x_0] \\ P_0 = E[(x_0 - \overline{x}_0)(x_0 - \overline{x}_0)^T] \end{cases} \tag{8}$$

where $E[\cdot]$ denotes the mean of $[\cdot]$
UKF-II: **Sigma Points Calculation in the *k*-th time instant**

$$\chi_{k-1} = \left[\overline{x}_{k-1}, \overline{x}_{k-1} + \sqrt{(L+\lambda)P_{k-1}}, \overline{x}_{k-1} - \sqrt{(L+\lambda)P_{k-1}} \right] \tag{9}$$

UKF-III: **Time Update**

$$\begin{cases} \chi_{k|k-1}^* = f(\chi_{k-1}) \\ \overline{x}_{k|k-1} = \sum_{i=0}^{2L} w_i^m \chi_{i,k|k-1}^* \\ P_{k|k-1} = \sum_{i=0}^{2L} w_i^c (\chi_{i,k|k-1}^* - \overline{x}_{k|k-1})(\chi_{i,k|k-1}^* - \overline{x}_{k|k-1})^T + Q^w \\ \chi_{k|k-1} = \left[\overline{x}_{k|k-1}, \overline{x}_{k|k-1} + \sqrt{(L+\lambda)P_{k|k-1}}, \overline{x}_{k|k-1} - \sqrt{(L+\lambda)P_{k|k-1}} \right] \\ \gamma_{k|k-1} = h(\chi_{k|k-1}) \\ \overline{y}_{k|k-1} = \sum_{i=0}^{2L} w_i^m \gamma_{i,k|k-1} \end{cases} \tag{10}$$

UKF-IV: **Measurement Update**

$$\begin{cases} P_{\bar{y}_k\bar{y}_k} = \sum_{i=0}^{2L} w_i^c (\gamma_{i,k|k-1} - \bar{y}_{k|k-1})(\gamma_{i,k|k-1} - \bar{y}_{k|k-1})^T + Q^v \\ P_{\bar{x}_k\bar{y}_k} = \sum_{i=0}^{2L} w_i^c (\chi_{i,k|k-1} - \bar{x}_{k|k-1})(\gamma_{i,k|k-1} - \bar{y}_{k|k-1})^T \\ K_k = P_{\bar{x}_k\bar{y}_k} P_{\bar{y}_k\bar{y}_k}^{-1} \\ P_k = P_{k|k-1} - K_k P_{\bar{y}_k\bar{y}_k} K_k^T \\ \bar{x}_k = \bar{x}_{k|k-1} + K_k (y_k - \bar{y}_{k|k-1}) \end{cases} \tag{11}$$

where Q^w and Q^v are the process and measurement noise covariance respectively, both of which are assumed to be known as *a priori*. The parameter a is usually set within [0.0001, 1].

3. MIT-AUKF

It is the same as KF to a linear system, UKF suffers performance degradation or even losing stability if the *a priori* knowledge of Q^w and Q^v in Eq.(10) and Eq.(11) mismatches the relative ones in real system denoted as R_w and R_v in the following sections. To avoid this problem, a MIT-rule-based approach is introduced in this section.

3.1 Parameters to be turned adaptively

From the previous introduction, there are six parameters need to be selected in UKF, including the initial state x_0, initial covariance P_0, process noise covariance Q^w, measurement noise covariance Q^v, and UT parameters a and β. The x_0 and P_0, however, usually have asymptotically negligible influence on the estimation results as more data are handled with time proceeding. And the values of a and β only affect the higher order terms of the nonlinear estimation but have little relation with the estimation accuracy or stability of UKF. Thus, the covariance matrices Q^w and Q^v are the only possible parameters which the adaptive law could update for improving the performance of UKF. Indeed, the selection of Q^w and Q^v does have significant influence on UKF. If Q^w and/or Q^v are too small at the beginning of the estimation process, the uncertainty tube around the estimated value will probably tighten and a biased solution might appear. On the other hand, too large Q^w and/or Q^v will probably result in filter divergence.

In this section, the adaptive UKF adjusting the process noise covariance Q^w will be introduced. And without losing the generality, the case of adjusting Q^v can be conducted in a similar way.

3.2 Cost function

In order to update the Q^w in time, most adaptive filters tried to minimize the time-averaged innovations, i.e., the measured outputs and their estimated values. However, the computation of minimum innovations is time consuming and the results may be different from the 'true' values. Here, we propose a recursive algorithm to minimize the difference between the filter-computed and the actual innovation covariance.

The time-averaged approximation of innovation covariance is defined as

$$S_k = \frac{1}{N}\sum_{i=k-N}^{k-1} v_i v_i^T \tag{12}$$

where N is the size of the estimation window, v_i is the innovation and can be written as,

$$v_i = y_i - \overline{y}_{i|i-1} \tag{13}$$

where y_i and $\overline{y}_{i|i-1}$ are respectively, the real measurement and its estimated value. From Eq.(11) of the standard UKF, the computed innovation covariance can be obtained as,

$$\hat{S}_k = P_{\overline{y}_k \overline{y}_k} = \sum_{i=0}^{2L} w_i^c (\gamma_{i,k|k-1} - \overline{y}_{k|k-1})(\gamma_{i,k|k-1} - \overline{y}_{k|k-1})^T + Q^v \tag{14}$$

Then, the criterion for adaptive UKF is to minimize the following cost function,

$$V_k = tr(\Delta S_k^2) = tr\left[(S_k - \hat{S}_k)^2\right] \tag{15}$$

3.3 MIT-AUKF algorithm

The MIT rule is used in this section to derive the adaptive law. With the MIT rule, the parameters are adjusted in the negative gradient direction of the criterion function, i.e.,

$$\dot{q}_k^m = -\eta_k \frac{\partial V_k}{\partial q_k^m} \tag{16}$$

where q_k^m is the m-th diagonal element of the process-noise covariance matrix at time k, i.e.,

$$Q_k^w = \begin{bmatrix} q_k^1 & \cdots & 0 \\ \vdots & \ddots & \vdots \\ 0 & \cdots & q_k^n \end{bmatrix}$$

and η is the tuning rate that determines the convergence speed, and it is assumed to satisfy the following conditions,

$$q_k^m = q_{k-1}^m - \eta_k \frac{\partial J_k}{\partial q_k^m} \cdot T \tag{17}$$

Eq.(16) leads to the following recursive scheme with respect to discrete time application,

$$q_k^m = q_{k-1}^m - \eta \frac{\partial V_k}{\partial q_{k-1}^m} \cdot T \tag{18}$$

where T is the sampling time. In order to calculate Eq. (18), the partial derivative of V_k with respect to q_k^m needs to be calculated. From Eq. (15), we have

$$\frac{\partial V_k}{\partial q_{k-1}^m} = \frac{\partial}{\partial q_{k-1}^m}\left(\sum_{i=1}^{m}\left(\Delta S_k\right)_{i,:}\left(\Delta S_k\right)_{:,i}\right) = \sum_{i=1}^{m}\left[\left(\frac{\partial\left(\Delta S_k\right)_{i,:}^T}{\partial q_{k-1}^m}\right)^T\left(\Delta S_k\right)_{:,i} + \left(\Delta S_k\right)_{i,:}\frac{\partial\left(\Delta S_k\right)_{:,i}}{\partial q_{k-1}^m}\right] \tag{19}$$

$$\frac{\partial\left(\Delta S_k\right)_{i,:}^T}{\partial q_{k-1}^m} = \frac{\partial\left(\Delta S_k\right)_{:,i}}{\partial q_{k-1}^m} = \frac{\partial}{\partial q_{k-1}^m}\left[\left(S_k\right)_{:,i} - \left(\hat{S}_k\right)_{:,i}\right] = \frac{\partial\left(S_k\right)_{:,i}}{\partial q_{k-1}^m} - \frac{\partial\left(\hat{S}_k\right)_{:,i}}{\partial q_{k-1}^m} \tag{20}$$

where $(\Delta S_k)_{i,:}$ and $(\Delta S_k)_{:,j}$ denote the ith row and jth column of matrix ΔS_k respectively. From Eq.(12) and (13), the first term of Eq.(20) is obtained as follows,

$$\frac{\partial(S_k)_{:,i}}{\partial q_{k-1}^m} = \frac{1}{N}\sum_{j=k-N+1}^{k}\left[-\frac{\partial(\overline{y}_{j|j-1,i})}{\partial q_{k-1}^m}(y_j - \overline{y}_{j|j-1})^T - (y_{j,i} - \overline{y}_{j|j-1,i})\frac{\partial(\overline{y}_{j|j-1}^T)}{\partial q_{k-1}^m}\right] \tag{21}$$

And the second term of Eq.(20) can be obtained from Eq.(14),

$$\frac{\partial(\hat{S}_k)_{:,i}}{\partial q_k^m} = \sum_{j=0}^{2n} w_i^c\left[-\frac{\partial\overline{y}_{k|k-1}}{\partial q_k^m}(\gamma_{j,k|k-1} - \overline{y}_{k|k-1})_{:,i}{}^T - (\gamma_{j,k|k-1} - \overline{y}_{k|k-1})\frac{\partial\overline{y}_{k|k-1,i}^T}{\partial q_k^m}\right] \tag{22}$$

Thus, the recursive algorithm for the gradient of innovation vector (InV) can be formulated as follows,

InV-I: **Initialization**

$$\begin{cases}\dfrac{\partial\overline{x}_0}{\partial q_k^m} = 0 \\ \dfrac{\partial P_0}{\partial q_k^m} = 0\end{cases} \tag{23}$$

InV-II: **Derivative of Sigma Points**

$$\begin{cases} \dfrac{\partial \chi_{0,k-1}}{\partial q_{k-1}^m} = \dfrac{\partial \overline{x}_{k-1}}{\partial q_{k-1}^m} \\ \dfrac{\partial \chi_{i,k-1}}{\partial q_{k-1}^m} = \dfrac{\partial \overline{x}_{k-1}}{\partial q_{k-1}^m} + \sqrt{L+\lambda} \cdot (\dfrac{\partial \sqrt{P_{k-1}}}{\partial q_{k-1}^m})_i, \quad i = 1,\ldots,L \\ \dfrac{\partial \chi_{i,k-1}}{\partial q_{k-1}^m} = \dfrac{\partial \overline{x}_{k-1}}{\partial q_{k-1}^m} - \sqrt{L+\lambda} \cdot (\dfrac{\partial \sqrt{P_{k-1}}}{\partial q_{k-1}^m})_{i-n}, i = L+1,\ldots,2L \end{cases} \tag{24}$$

InV-III: **Derivative Propagation**

$$\begin{cases} \dfrac{\partial \chi_{i,k|k-1}^*}{\partial q_{k-1}^m} = \left.\dfrac{\partial f}{\partial x}\right|_{x=\chi_{i,k-1}} \cdot \dfrac{\partial \chi_{i,k-1}}{\partial q_{k-1}^m} \\ \dfrac{\partial \overline{x}_{k|k-1}}{\partial q_{k-1}^m} = \sum_{i=0}^{2L} w_i^m \dfrac{\partial \chi_{i,k|k-1}^*}{\partial q_{k-1}^m} \\ \dfrac{\partial P_{k|k-1}}{\partial q_{k-1}^m} = \sum_{i=0}^{2L} w_i^c \left\{ \left(\dfrac{\partial \chi_{i,k|k-1}^*}{\partial q_{k-1}^m} - \dfrac{\partial \overline{x}_{k|k-1}}{\partial q_{k-1}^m} \right) (\chi_{i,k|k-1}^* - \overline{x}_{k|k-1})^T + \right. \\ \qquad \left. (\chi_{i,k|k-1}^* - \overline{x}_{k|k-1}) \left(\dfrac{\partial \chi_{i,k|k-1}^*}{\partial q_{k-1}^m} - \dfrac{\partial \overline{x}_{k|k-1}}{\partial q_{k-1}^m} \right)^T \right\} \end{cases} \tag{25a}$$

$$\begin{cases} \dfrac{\partial \chi_{0,k|k-1}}{\partial q_{k-1}^m} = \dfrac{\partial \overline{x}_{k|k-1}}{\partial q_{k-1}^m} \\ \dfrac{\partial \chi_{i,k|k-1}}{\partial q_{k-1}^m} = \dfrac{\partial \overline{x}_{k|k-1}}{\partial q_{k-1}^m} + \sqrt{L+\lambda} (\dfrac{\partial \sqrt{P_{k|k-1}}}{\partial q_{k-1}^m})_i, \quad i = 1,\ldots,L \\ \dfrac{\partial \chi_{i,k|k-1}}{\partial q_{k-1}^m} = \dfrac{\partial \overline{x}_{k|k-1}}{\partial q_{k-1}^m} - \sqrt{L+\lambda} (\dfrac{\partial \sqrt{P_{k|k-1}}}{\partial q_{k-1}^m})_{i-n}, i = L+1,\ldots,2L \end{cases} \tag{25b}$$

InV-IV: **Interested Derivative**

$$\begin{cases} \dfrac{\partial \gamma_{i,k|k-1}}{\partial q_{k-1}^m} = \left.\dfrac{\partial h}{\partial x}\right|_{x=\chi_{i,k|k-1}} \cdot \dfrac{\partial \chi_{i,k|k-1}}{\partial q_{k-1}^m} \\ \dfrac{\partial \overline{y}_{k|k-1}}{\partial q_{k-1}^m} = \sum_{i=0}^{2L} w_i^m \dfrac{\partial \gamma_{i,k|k-1}}{\partial q_{k-1}^m} \end{cases} \tag{26}$$

***InV-V:* Derivative Update**

$$
\begin{cases}
\dfrac{\partial P_{k|k-1}}{\partial q_k^m} = I \\
\dfrac{\partial \chi_{i,k|k-1}}{\partial q_k^m} = \sqrt{L+\lambda}\left(\dfrac{\partial \sqrt{P_{k|k-1}}}{\partial q_k^m}\right)_i, \quad i = 1,\ldots,L \\
\dfrac{\partial \chi_{i,k|k-1}}{\partial q_k^m} = -\sqrt{L+\lambda}\left(\dfrac{\partial \sqrt{P_{k|k-1}}}{\partial q_k^m}\right)_{i-n}, i = L+1,\ldots,2L \\
\dfrac{\partial \gamma_{i,k|k-1}}{\partial q_k^m} = \left.\dfrac{\partial h}{\partial x}\right|_{x=\chi_{i,k|k-1}} \cdot \dfrac{\partial \chi_{i,k|k-1}}{\partial q_k^m} \\
\dfrac{\partial \overline{y}_{k|k-1}}{\partial q_k^m} = \sum_{i=0}^{2L} w_i^m \dfrac{\partial \gamma_{i,k|k-1}}{\partial q_k^m} \\
\dfrac{\partial P_{\overline{y}_k\overline{y}_k}}{\partial q_k^m} = \sum_{i=0}^{2L} w_i^c \left\{ \left(\dfrac{\partial \gamma_{i,k|k-1}}{\partial q_k^m} - \dfrac{\partial \overline{y}_{k|k-1}}{\partial q_k^m} \right) (\gamma_{i,k|k-1} - \overline{y}_{k|k-1})^T \right. \\
\qquad \left. + (\gamma_{i,k|k-1} - \overline{y}_{k|k-1}) \left(\dfrac{\partial \gamma_{i,k|k-1}}{\partial q_k^m} - \dfrac{\partial \overline{y}_{k|k-1}}{\partial q_k^m} \right)^T \right\} + \dfrac{\partial Q^w}{\partial q_k^m} \\
\dfrac{\partial P_{\overline{x}_k\overline{y}_k}}{\partial q_k^m} = \sum_{i=0}^{2L} w_i^c \left\{ \left(\dfrac{\partial \chi_{i,k|k-1}}{\partial q_k^m} - \dfrac{\partial \overline{x}_{k|k-1}}{\partial q_k^m} \right) (\gamma_{i,k|k-1} - \overline{y}_{k|k-1})^T \right. \\
\qquad \left. + (\chi_{i,k|k-1} - \overline{x}_{k|k-1}) \cdot \left(\dfrac{\partial \gamma_{i,k|k-1}}{\partial q_k^m} - \dfrac{\partial \overline{y}_{k|k-1}}{\partial q_k^m} \right)^T \right\}
\end{cases}
\tag{27a}
$$

$$
\begin{cases}
\dfrac{\partial K_k}{\partial q_k^m} = \dfrac{\partial P_{\overline{x}_k\overline{y}_k}}{\partial q_k^m} P_{\overline{y}_k\overline{y}_k}^{-1} - P_{\overline{x}_k\overline{y}_k} P_{\overline{y}_k\overline{y}_k}^{-1} \dfrac{\partial P_{\overline{y}_k\overline{y}_k}}{\partial q_k^m} P_{\overline{y}_k\overline{y}_k}^{-1} \\
\dfrac{\partial P_k}{\partial q_k^m} = \dfrac{\partial P_{k|k-1}}{\partial q_k^m} - \dfrac{\partial K_k}{\partial q_k^m} P_{\overline{x}_k\overline{y}_k}^T - K_k \left(\dfrac{\partial P_{\overline{x}_k\overline{y}_k}}{\partial q_k^m} \right)^T \\
\dfrac{\partial \overline{x}_k}{\partial q_k^m} = \dfrac{\partial \overline{x}_{k|k-1}}{\partial q_k^m} + \dfrac{\partial K_k}{\partial q_k^m} (y_k - \overline{y}_{k|k-1}) - K_k \dfrac{\partial \overline{y}_{k|k-1}}{\partial q_k^m}
\end{cases}
\tag{27b}
$$

where

$$
P_{k|k-1} = \sum_{i=0}^{2L} w_i^c (\chi_{i,k|k-1}^* - \overline{x}_{k|k-1})(\chi_{i,k|k-1}^* - \overline{x}_{k|k-1})^T + Q_k^w
$$

Finally, the procedure of MIT-AUKF can be concluded as:

***MIT-AUKF-I:* Initialization**
Initialize the UKF algorithm from Eq.(8) and the gradient of Eq.(23), and let

$$\begin{cases} Q_0^w = \bar{Q}^w \\ Q^v = \bar{Q}^v \end{cases}$$

***MIT-AUKF-II:* Sigma Points Calculation at the *k*-th time instant**
Compute the sigma points as Eq.(9) and the derivative update of Eq.(24).
***MIT-AUKF-III:* Time Update**
Obtain the time update of UKF as Eq. (10) and compute the derivative update of Eq. (25).
***MIT-AUKF-IV:* Update Process Noise Covariance Matrix**
Compute the interested derivative with Eq.(26) and obtain new process noise covariance matrix by Eq.(18-22).
***UKF-IV:* Measurement Update**
Complete the measurement update as Eq.(11) and the last update of Eq.(27).

4. MS-AUKF

In the MIT-AUKF, the partial derivative of $\hat{S}_k$ with respect to q_k^m has to be calculated as Eq. (22), which will introduce a relative large computational burden. In this section, another AUKF scheme with master-slave structure is proposed with the purpose of avoiding the complicated calculation.
Shown in Fig.2, the proposed MS-AUKF is composed of two parallel UKFs. At every timestep, the master UKF estimates the states/parameters using the noise covariance obtained by the slave UKF, while the slave UKF estimates the noise covariance using the innovations generated by the master UKF. It should be noted that the two UKFs are independent in the MS-AUKF structure. Thus, the slave UKF can be replaced by another simple filter such as KF to save the computational burden in time-critical application.

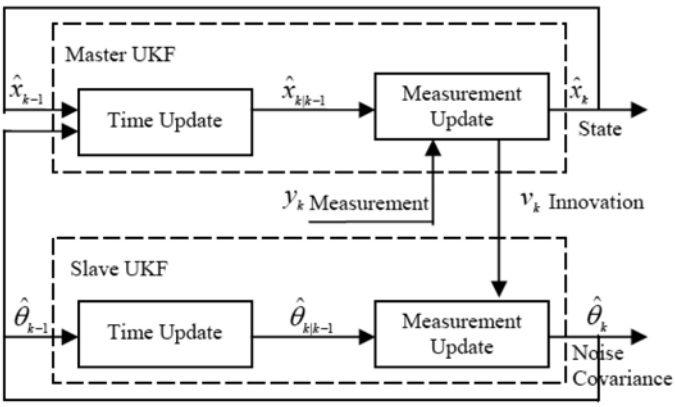

Fig. 2. The Structure of MS-AUKF

In the proposed scheme, the calculation of the master UKF is the same as that of a normal UKF. The slave UKF, on the other hand, needs to estimate the noise covariance. In this section, without losing the generality, the slave UKF is described to estimate the

measurement covariance matrix, here, we use the θ_k^i to denote the ith diagonal element of matrix Q_k^v, i.e.,

$$Q_k^v = \begin{bmatrix} \theta_k^1 & \cdots & 0 \\ \vdots & \ddots & \vdots \\ 0 & \cdots & \theta_k^m \end{bmatrix} \tag{28}$$

In the case that the dynamics of θ are clearly known, i.e.,

$$\theta_k = f\left(\theta_{k-1}\right) + w_{\theta k} \tag{29}$$

then Eq.(29) can be directly used as the reference model of the slave UKF. While the dynamics of θ are unknown, we can use a noise-actuated model like Eq.(30) instead.

$$\theta_k = \theta_{k-1} + w_{\theta k} \tag{30}$$

where $w_{\theta k}$ is supposed to be Gaussian white noise with zero mean.
The innovation covariance generated by the master UKF is taken as the observation signal for the slave UKF, and then according to Eq.(11), the observation model can be described as,

$$\overline{S}_k = g\left(\theta_k\right) = diag\left[\sum_{i=0}^{2n} w_i^c (\gamma_{i,k|k-1} - \overline{y}_{k|k-1})(\gamma_{i,k|k-1} - \overline{y}_{k|k-1})^T + Q_{k-1}^v\right] \tag{31}$$

The measurement of $\hat{S}_k$ received by the slave UKF is,

$$S_k = diag\left[v_k v_k^T\right] \tag{32}$$

$$v_k = y_k - \overline{y}_{k|k-1} \tag{33}$$

where v_k is innovation, and y_k is the real measurements in Eq.(11).
Therefore, the recursive algorithm of the slave UKF can be formulated as,
Slave-I: **Initialization**

$$\begin{cases} \hat{\theta}_0 = E\left[\theta_0\right] \\ P_{\theta_0} = E\left[\left(\theta_0 - \hat{\theta}_0\right)\left(\theta_0 - \hat{\theta}_0\right)^T\right] \end{cases} \tag{34}$$

Slave-II: **Sigma Points Calculation**

$$\vartheta_{k-1} = [\hat{\theta}_{k-1}, \hat{\theta}_{k-1} + \sqrt{(1+\lambda)P_{\theta_{k-1}}}, \hat{\theta}_{k-1} - \sqrt{(1+\lambda)P_{\theta_{k-1}}}] \tag{35}$$

Slave-III: **Time Update**

$$\begin{cases} \vartheta_{k|k-1} = f_\theta(\vartheta_{k-1}) \\ \hat{\theta}_{k|k-1} = \sum_{i=0}^{2n} w_{\theta_i}^m \vartheta_{i,k|k-1}^* \\ P_{\theta_{k|k-1}} = \sum_{i=0}^{2n} w_{\theta_i}^m (\vartheta_{i,k|k-1}^* - \hat{\theta}_{k|k-1})(\vartheta_{i,k|k-1}^* - \hat{\theta}_{k|k-1})^T + Q^\theta \\ \vartheta_{k|k-1} = [\hat{\theta}_{k|k-1}, \hat{\theta}_{k|k-1} + \sqrt{(1+\lambda)P_{\theta_{k|k-1}}}, \hat{\theta}_{k|k-1} - \sqrt{(1+\lambda)P_{\theta_{k|k-1}}}] \\ \varsigma_{k|k-1} = g(\vartheta_{k|k-1}) \\ \hat{S}_{k|k-1} = \sum_{i=0}^{2n} w_{\theta_i}^m \varsigma_{i,k|k-1} \end{cases} \tag{36}$$

Slave-IV: **Measurement Update**

$$\begin{cases} P_{S_k S_k} = \sum_{i=0}^{2n} w_{\theta_i}^c (\varsigma_{i,k|k-1} - \hat{S}_{k|k-1})(\varsigma_{i,k|k-1} - \hat{S}_{k|k-1})^T + R^\theta \\ P_{\theta_k S_k} = \sum_{i=0}^{2n} w_{\theta_i}^c (\vartheta_{i,k|k-1} - \hat{\theta}_{k|k-1})(\vartheta_{i,k|k-1} - \hat{\theta}_{k|k-1})^T + R^\theta \\ K_{\theta_k} = P_{\theta_k S_k} P_{S_k S_k}^{-1} \\ \hat{\theta}_k = \hat{\theta}_{k|k-1} + K_{\theta_k}(S_k - \hat{S}_{k|k-1}), \quad P_{\theta_k} = P_{\theta_{k|k-1}} - K_{\theta_k} P_{S_k S_k} K_{\theta_k}^T \end{cases} \tag{37}$$

where Q^θ and $R^\theta$are respectively the process and measurement noise covariance matrix, and the weights can be calculated by Eq.(6).
Finally, the procedure of the MS-AUKF can be easily obtained by directly combining the four steps of UKF as Eq.(8) – (11) and the slave UKF as Eq.(34) – (37).

5. Application of AUKF

In this section, we introduce the applications of the proposed AUKFs on the dynamics of both a ground mobile robot and a model helicopter, to demonstrate the performance of the AUKFs in state/parameter estimation and control.

5.1 State estimation

First, the simulations of applying the two AUKFs to state estimation are conducted with respect to the dynamics of the omni-directional ground mobile robot developed in Shenyang Institute of Automation, CAS (See Fig. 3) (Song, 2002),

$$\begin{cases} (2Mr^2 + 3i_n I_w)\ddot{x}_w + 3i_n^2 I_w \dot{y}_w \dot{\varphi}_w + 3i_n^2 c\dot{x}_w = nr(\beta_1 u_1 + 2u_2 \cos\varphi_w + \beta_2 u_3) \\ (2Mr^2 + 3i_n I_w)\ddot{y}_w - 3i_n^2 I_w \dot{x}_w \dot{\varphi}_w + 3i_n^2 c\dot{y}_w = nr(\beta_3 u_1 + 2u_2 \sin\varphi_w + \beta_4 u_3) \\ (3i_n I_w L^2 + I_v r^2)\ddot{\varphi}_w + 3i_n^2 cL^2 \dot{\varphi}_w = nrL(-u_1 - u_2 - u_3) \end{cases} \tag{38}$$

$$\begin{cases} \beta_1 = -\sqrt{3}\sin\varphi_w - \cos\varphi_w \\ \beta_2 = \sqrt{3}\sin\varphi_w - \cos\varphi_w \\ \beta_4 = -\sqrt{3}\cos\varphi_w - \sin\varphi_w \\ \beta_3 = \sqrt{3}\cos\varphi_w - \sin\varphi_w \end{cases} \tag{39}$$

where x_w, y_w, and φ_w respectively represent the displacements in the x-, y-direction and the rotation; u_1, u_2, and u_3 are the actuated torques on each joint. Other parameters in Eq. (38) and Eq. (39) are listed in Table 1.

Fig. 3. 3-DOF Omni-Directional Mobile Robot

Symbols	Physical Meanings	Values in Simulations
c	Friction Coefficient	0.0009kgm2/s
Iw	Inertia on motor axis	0.0036 kgm2
M	Mass	120kg
Iv	Inertia	45 kgm2
r	Wheel Radius	0.06m
L	Centroid-wheel distance	0.273m
in	Motor gear radio	15

Table 1. Mobile Robot Parameters

The state and measurement vectors are selected as follows,

$$\begin{cases} \bar{x} = [x_w, y_w, \phi_w, \dot{x}_w, \dot{y}_w, \dot{\phi}_w]^T \\ y = [\dot{x}_w, \dot{y}_w, \dot{\phi}_w]^T \end{cases} \tag{40}$$

The sampling interval is set as T=0.01s. During the simulation, measurements are corrupted by an zero mean white noise with covariance R_v = diag{10^{-8}; 10^{-8}; 10^{-8}}. The UKF parameters are designed as,

$$\begin{cases} \hat{x}_0 = x_{T_0} \\ \hat{P}_0 = diag\{10^{-8}, 10^{-8}, 10^{-8}, 10^{-8}, 10^{-8}, 10^{-8}\} \\ Q^v = R_v \\ \alpha = 1 \\ \beta = 2 \end{cases} \tag{41}$$

In order to demonstrate the performance of the AUKFs, we assume an abrupt change occurring with the process noise at the time of t=10s, i.e., the *a priori* knowledge is no longer match the real one after t=10s,

$$R_w = \begin{cases} diag\{10^{-12}, 10^{-12}, 10^{-12}, 10^{-8}, 10^{-8}, 10^{-8}\} & t < 10s \\ diag\{10^{-10}, 10^{-10}, 10^{-10}, 10^{-6}, 10^{-6}, 10^{-6}\} & t \geq 10s \end{cases} \tag{42}$$

In all of the three UKFs, i.e., the normal UKF, MIT-AUKF and MS-AUKF, the *a priori* process noise covariance is set as Q = diag{10^{-12}, 10^{-12}, 10^{-12}, 10^{-8}, 10^{-8}, 10^{-8}}.
The velocity estimation errors of the three UKFs, under the same noise change of Eq.(42) at t =10s, are illustrated in Fig. 4, where the parameters required by the MIT-AUKF and MSAUKF are respectively selected as Eq.(43) and (44),

$$\eta = 10^{-12} \tag{43}$$

$$\begin{cases} \theta_0 = \left[10^{-12}, 10^{-12}, 10^{-12}, 10^{-8}, 10^{-8}, 10^{-8}\right]^T \\ P_{\theta_0} = diag\left\{10^{-16}, 10^{-16}, 10^{-16}, 10^{-16}, 10^{-16}, 10^{-16}\right\} \\ Q_\theta^w = diag\left\{10^{-24}, 10^{-24}, 10^{-24}, 10^{-21}, 10^{-21}, 10^{-21}\right\} \\ Q_\theta^n = diag\left\{2\times10^{-16}, 2\times10^{-16}, 2\times10^{-16}\right\} \end{cases} \tag{44}$$

From Fig. 4, we can see that, with incorrect *a priori* noise statistic information, the normal UKF can not produce satisfying estimations due to the violation of the optimality conditions. On the contrary, the estimation errors of the two proposed AUKF are quickly convergent due to the performance of the adaptive laws.

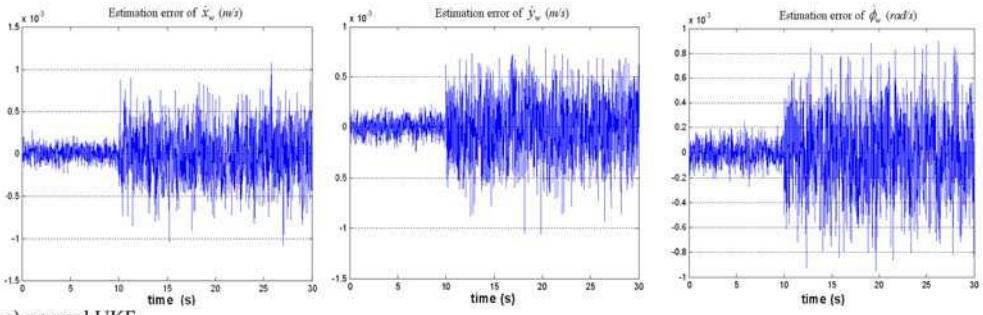

a) normal UKF

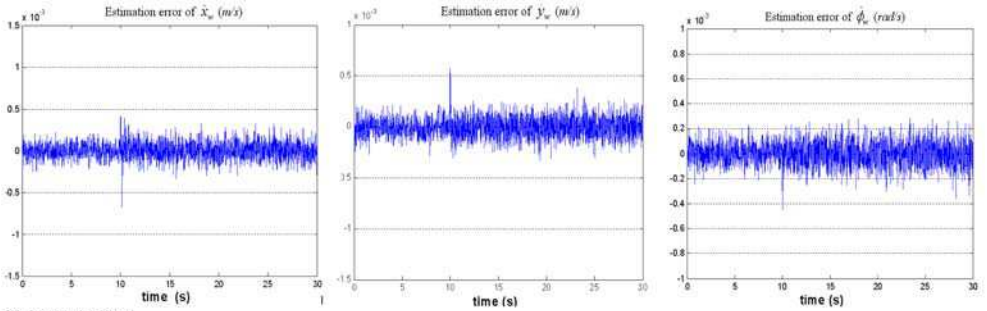

b) MIT-AUKF

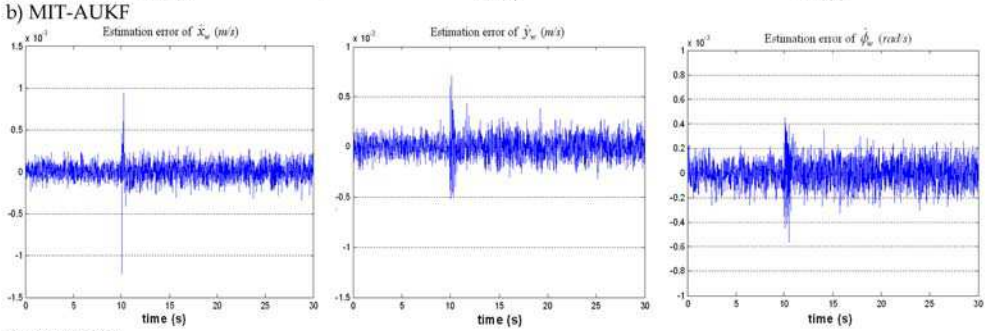

c) MS-AUKF

Fig. 4. Velocity Estimation Errors With Respect To Changing Process Noise Covariance

5.2 Performance comparison

In this section, we compare the performance of the three UKFs in two aspects: 1) estimation precision, and 2) computational time. In order to quantify the estimation precision, the following criterion is defined,

$$J_{ac} = \sqrt{\frac{1}{N_k}\sum_{k=1}^{N_k}(x_k - \overline{x}_k)^2} \tag{45}$$

where N_k is the number of sample points, x_k is the real state or parameter, $\overline{x}_k$ is the estimated state or parameter.

		Normal UKF	MIT-AUKF	MS-AUKF
Computational Time		8.83	45.52	14.94
After the changing of the process noise covariance	ER of $\dot{x}_w$	0.00020	0.000070	0.000079
	ER of $\dot{y}_w$	0.00021	0.000071	0.000076
	ER $\dot{\varphi}_w$	0.00020	0.000071	0.000076

*ER means Estimation error

Table 2. Performance comparison of the two AUKFs

Table-2 shows the performance comparison of the three AUKFs, where the unit of the computational time has been ignored since the simulations are conducted by MATLAB, but the ratio among the three can indicate the complexity of AUKF with respect to that of the normal UKF. From Table-2, we can conclude that: 1) the computational time of the MSAUKF is almost one-third of that of MIT-AUKF, but one times longer than that of normal UKF because two UKFs have to be calculated in the MS-UKF. The accuracy of the MS-AUKF is about 2.5 times higher than that of normal UKF. The MIT-AUKF, although suffering from the most complicated computation, achieves the best accuracy among the three UKFs, and about 7% more accuracy than that of MS-AUKF.

5.3 Disturbance estimation

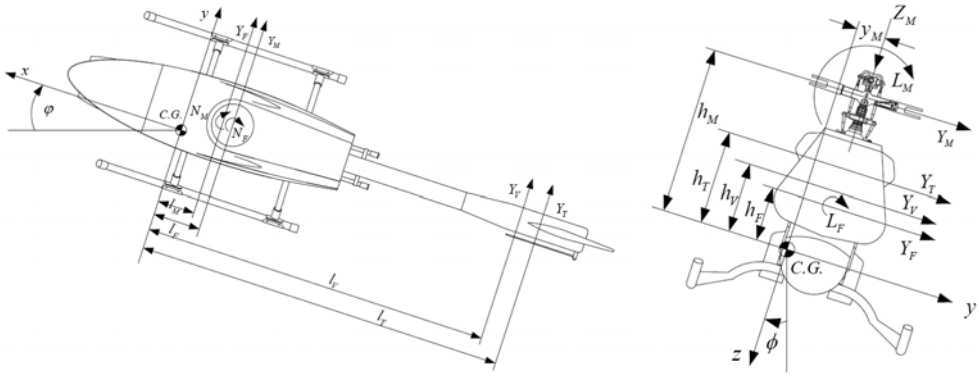

(a)Planform (b) Back view

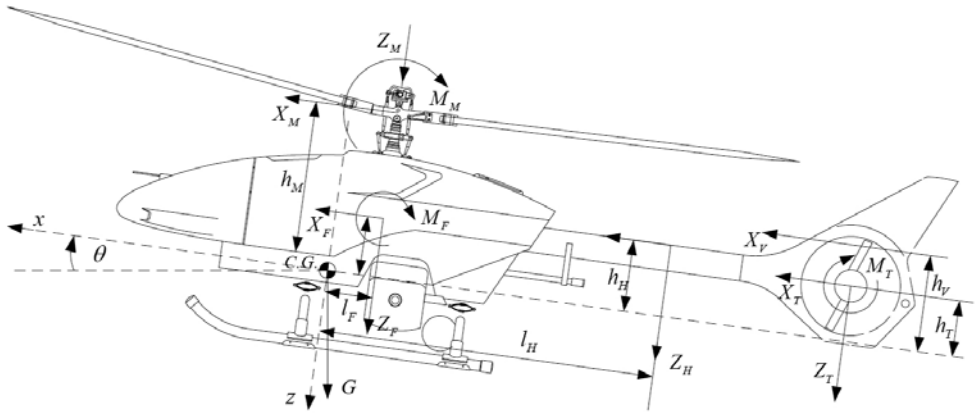

(c) Side view

Fig. 5. Model Helicopter

In this section, we investigate the disturbance and state estimation of an unmanned helicopter. The dynamics of a model helicopter can be described as (see Fig.5, and Koo & Sastry, 1998; He & Han, 2007),

$$\begin{bmatrix} \dot{p} \\ \dot{v}^p \\ \dot{\Theta} \\ \dot{\omega}^b \end{bmatrix} = \begin{bmatrix} v^p \\ \frac{1}{m} W f^b \\ \Psi \omega^b \\ J^{-1}(\tau^b - \omega^b \times J\omega^b) \end{bmatrix} \tag{46}$$

$$\begin{aligned} f^b &= \begin{bmatrix} -T_M \sin a_{1s} \\ T_M \sin b_{1s} + T_T \\ -T_M \cos a_{1s} \cos b_{1s} \end{bmatrix} + W^T \begin{bmatrix} 0 \\ 0 \\ mg \end{bmatrix} + \Delta_1 \\ \tau^b &= \begin{bmatrix} S_{L_1} b_{1s} + S_{L_2} Q_M \\ S_{M_1} a_{1s} + S_{M_2} T_M + S_{M_3} Q_T \\ S_{N_1} Q_M + S_{N_2} T_T \end{bmatrix} + \begin{bmatrix} T_M \sin b_{1s} h_M - T_M \cos a_{1s} \cos b_{1s} y_M + T_T h_T \\ T_M \sin a_{1s} h_M - T_M \cos a_{1s} \cos b_{1s} l_M \\ -T_M \sin b_{1s} l_M - T_T l_T \end{bmatrix} + \Delta_2 \end{aligned} \tag{47}$$

where $p \in R^3$ and $v_p \in R^3$ are the position and velocity vector of the center of mass in inertia frame; $W \in SO(3)$ is the rotation matrix of the body frame relative to the inertia frame; ω_b is angular velocity vector; $\Theta = [\varphi\ \theta\ \psi]^T$ is Euler angle vector; m and J are respectively, the mass and inertia of the helicopter; Ψ is the transformation matrix from angular velocity to angular position; f^b and τ^b are force and moment acted on the helicopter in body frame including disturbances; the subscript M and T denote the main and tail rotor respectively; T and Q are respectively, the force and torque generated by main or tail rotor; a_{1s} and b_{1s}, are respectively, the longitudinal and lateral tilt of the tip path plane of the main rotor with respect to shaft; h_M, y_M, h_T, l_M, l_T are constants indicating the distances as Fig.5; Δ_1 and Δ_2 denote the unmodeled dynamics.

The forces T and the moments Q in Eq. (47) can be further calculated by

$$\begin{aligned} T_i &= \frac{R_{1i}^3 - R_{0i}^3}{3} m_3 \theta_{ci} + \frac{m_3 m_6}{2}\left(R_{1i}^2 - R_{0i}^2\right) - \frac{m_3}{8\pi\Omega_1^2}\{\frac{2}{15 m_2^2 \theta_{ci}^2} \times \\ &\quad \left(\left(3m_2 R_{1i}\theta_{ci} - 2m_5\right)\left(m_2 R_{1i}\theta_{ci} + m_5\right)^{3/2} - \left(3m_2 R_{0i}\theta_{ci} - 2m_5\right)\left(m_2 R_{0i}\theta_{ci} + m_5\right)^{3/2}\right)\} \\ Q_i &= n_1 n_7 \frac{R_{1i}^3 - R_{0i}^3}{3} - \frac{n_1 n_9}{2}\left(R_{1i}^3 - R_{0i}^3\right) + \frac{c_d n_1}{4}\left(R_{1i}^4 - R_{0i}^4\right) + \\ &\quad \frac{2 n_1 n_8}{105 m_4^3}\left\{\left(15 m_4^2 R_{1i}^2 - 12 m_4 m_5 R_{1i} + 8 m_5^2\right)\left(m_4 R_{1i} + m_5\right)^{3/2} - \right. \\ &\quad \left.\left(15 m_4^2 R_{0i}^2 - 12 m_4 m_5 R_{0i} + 8 m_5^2\right)\left(m_4 R_{0i} + m_5\right)^{3/2}\right\} + \\ &\quad \frac{2 n_1 n_{10}}{15 m_4^3}\left\{\left(\left(3m_2 R_{1i} - 2m_5\right)\left(m_2 R_{1i} + m_5\right)^{3/2} - \right.\right. \\ &\quad \left.\left.\left(3m_2 R_{0i} - 2m_5\right)\left(m_2 R_{0i} + m_5\right)^{3/2}\right)\right\} \end{aligned} \tag{48}$$

where m_1~m_6, n_1~n_{10} are aerodynamics-related coefficients and the detailed description can be found in reference (Shim, 2000). These coefficients are time-varying and can not be accurately determined.

It can be seen that the complete dynamics of Eq.(48) is too complicated to be used for controller design. Hence, it has to be simplified before using as a reference model of control. But the simplification will definitely introduce extra uncertainties besides the aerodynamics related disturbances, both of which need the controller to handle and overcome. One of the simplified models of aerodynamics-generated force/torque is like,

$$
\begin{aligned}
f^b &= \begin{bmatrix} -T_M a_{1s} \\ T_M b_{1s} + T_T \\ -T_M \end{bmatrix} + R^T \begin{bmatrix} 0 \\ 0 \\ mg \end{bmatrix} + \Delta_1 \\
\tau^b &= \begin{bmatrix} S_{L1} b_{1s} + S_{L2} Q_M + T_M b_{1s} h_M - T_M y_M + T_T h_T \\ S_{M1} a_{1s} + S_{M2} T_M + S_{M3} Q_T + T_M a_{1s} h_M - T_M l_M \\ S_{N1} Q_M + S_{N2} T_T + -T_M b_{1s} l_M - T_T l_T \end{bmatrix} + \Delta_2 \\
T_M &= S_{T_M 1}\theta_M + S_{T_M 2},\ T_T = S_{T_T}\theta_T + S_{T_T 2},\ Q_M = S_{Q_M 1}\theta_M + S_{Q_M 2},\ Q_T = S_{Q_T}\theta_T + S_{Q_T 2}
\end{aligned}
\tag{49}
$$

And in the following simulation, we use the proposed MIT-AUKF algorithm to estimate the system states and the modeling error, and the estimated results are further used in an adaptive controller to attenuate the influence of uncertainties and disturbances in section 5.4. The simulation is conducted on the yaw dynamics of Eq.(50), which can be obtained by Eq.(46)-(49) (Song & Han, 2007),

$$
\ddot{\psi} = a_1\dot{\psi} + a_2\dot{\psi}^2 + b_1(S_{M_1} a_{1s} + S_{M_2} T_M + S_{M_3} Q_T) + b_2(S_{N_1} Q_M + S_{N_2} T_T) + b_3 \tag{50}
$$

where

$$
\begin{aligned}
\ddot{\psi} &= a_1\psi + a_2\dot{\psi} + b_1(S_{M_1} a_{1s} + S_{M_2} T_M + S_{M_3} Q_T) + b_2(S_{N_1} Q_M + S_{N_2} T_T) + b_3 \\
a_1 &= (\dot{\phi}\sin\phi\cos\phi - \dot{\theta}\sin^2\phi\cos\phi)(I_x - I_y)/I_z + \dot{\theta}\tan\theta - \\
&\qquad (\dot{\theta}\cos^2\phi\tan\phi + \dot{\phi}\sin\phi\cos\phi)(I_y - I_x)/I_z \\
a_2 &= \sin\theta\sin\phi\cos\phi(I_y - I_x)/I_z - \sin\theta\sin\phi\cos\phi(I_x - I_z)/I_y \\
b_1 &= \sin\phi\sec\theta/I_y \\
b_2 &= \cos\phi\sec\theta/I_z \\
b_3 &= \dot{\theta}\dot{\phi}(\sin^2\phi\sec\theta(I_x - I_z)/I_y + \cos^2\phi\sec\theta(I_y - I_x)/I_z + \sec\theta)
\end{aligned}
$$

The state and the measurement vector of AUKF are selected as,

$$
\begin{cases} x = [\psi \quad \dot{\psi}] \\ y = [\psi \quad \dot{\psi}] \end{cases} \tag{51}
$$

The sampling interval is T=0.02s. The measurements are corrupted by a zero mean additive white noise with covariance,

$$R_v = diag\{10^{-10}, 10^{-10}\} \tag{52}$$

The AUKF parameters are selected as,

$$\begin{cases} x_0 = x_{T_0} \\ \hat{P}_0 = diag\{10^{-14}, 10^{-10}\} \\ Q^v = R_v \\ a = 1, \beta = 1 \end{cases} \tag{53}$$

$$\eta = \begin{bmatrix} 10^{-25} & 0 & 0 \\ 0 & 10^{-25} & 0 \\ 0 & 0 & 10^{-20} \end{bmatrix}$$

Assume an abrupt change occuring with respect to the process noise covariance at t=10s, i.e.,

$$Q_t = \begin{cases} diag\{10^{-14}, 10^{-10}\} & t < 10s \\ diag\{10^{-12}, 10^{-8}\} & t \geq 10s \end{cases} \tag{54}$$

while the prior knowledge remain unchanged during the estimation. The estimation results obtained by both the MIT-AUKF and normal UKF are presented in Fig. 6, where we can see that the state estimated by AUKF is not influenced by the noise covariance changed at t=10s. But for the state estimated by normal UKF, it starts to bias from its true value at t=10s.

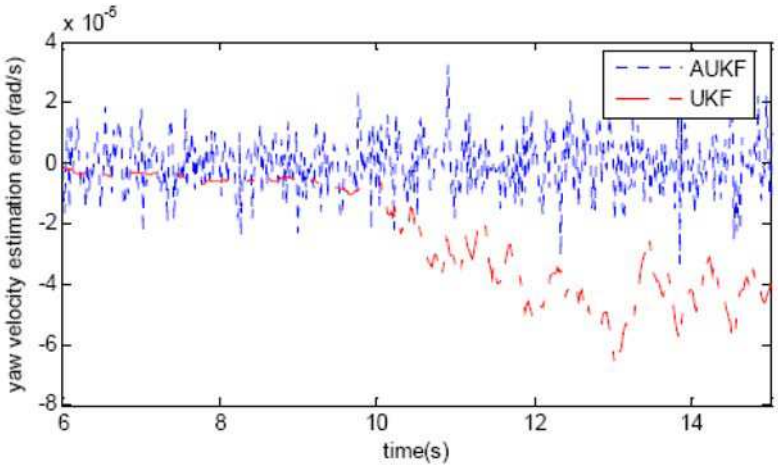

Fig. 6. State Estimation with Respect to Changing Process Noise Covariance

Besides the state estimation, parameter estimation is also tested and compared between the MIT-AUKF and normal UKF. In order to estimate the model error, an extended reference model is proposed as Eq.(55), where the model error is treated as an extra parameter driven by noise.

$$\begin{cases} \dot{\psi} = \dot{\psi} + w_1 \\ \ddot{\psi} = f(p_2, \dot{p}_2, \psi, \dot{\psi}, u) + \zeta + w_2 \\ \dot{\zeta} = w_3 \end{cases} \tag{55}$$

where $[\psi, \dot{\psi}, \zeta]^T$ is the vector to be estimated, and ζ presents model error plus disturbance, w_1, w_2 and w_3 are the process noises, $f(.)$ can be found in the following Eq. (59). By assuming that the model error changes at t = 10s, i.e.,

$$\begin{cases} \zeta = 0 & t < 6s \\ \zeta = 15.6 & t \geq 6s \end{cases} \tag{56}$$

and the state vector is subject to zero mean additive white noises with covariance,

$$Q_T^a = diag\{10^{-14}, 10^{-10}, 10^{-20}\} \tag{57}$$

Fig. 7 presents the results of disturbance estimation, from which we can see that the standard UKF cannot track the abrupt change due to the lower pseudonoise intensity. As for the adaptive UKF, the intensity of the pseudonoise increases during the parameter updates by the proposed adaptive mechanism. This accelerates the convergence of the model error estimation and makes the AUKF successfully track the abrupt change after a short period (about 1 second) of adaptation.

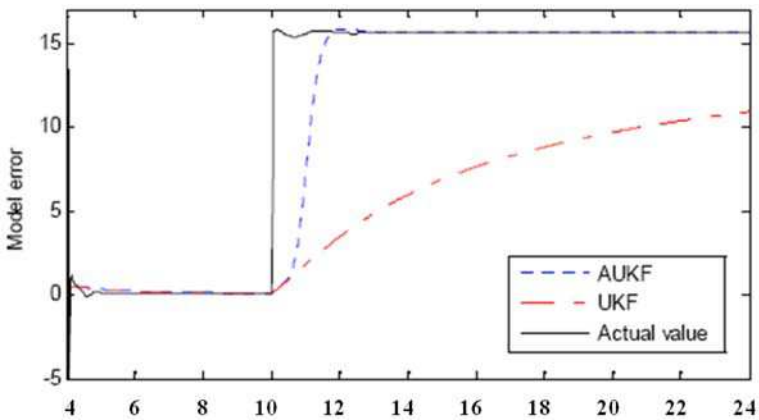

Fig. 7. Comparison of Disturbance Estimation When Noise Covariance Changing

5.4 Active estimation enhanced control

In order to design a tracking controller involving active estimation for robustness enhancement, we use the feedback linearization method to divide the helicopter dynamics into two parts: position dynamics and yaw dynamics. It can be proved that Eq.(46), (47) and (49) can be transformed into the following form (He & Han, 2007),

$$\begin{aligned} \ddot{p}_1 &= p_2 + \Delta_1 \\ \ddot{p}_2 &= f_2(p_1, \dot{p}_1, p_2, \dot{p}_2) + g_2(p_1, \dot{p}_1, p_2, \dot{p}_2)u + h_2(p_1, \dot{p}_1, p_2, \dot{p}_2)\Delta_2 \end{aligned} \tag{58}$$

$$\ddot{\psi} = f_3(p_2, \dot{p}_2, \psi, \dot{\psi}) + g_3(p_2, \dot{p}_2, \psi, \dot{\psi})u + \zeta \tag{59}$$

where Eq.(59) is the same as that in Eq. (55), and

$$f_2 = \frac{2\dot{T}_M}{M} R(\omega^b \times [0\ 0\ 1]^T) + \frac{T_M}{M} R[\omega^b \times (\omega^b \times [0\ 0\ 1]^T)] - \frac{T_M}{M} R\{[J^{-1}(\omega^b \times J\omega^b)] \times [0\ 0\ 1]^T\}$$

$$g_2 = \frac{1}{M}[T_M R\bar{J} \quad R[0\ 0\ 1]^T]; h_2 = \frac{T_M}{M} R\bar{J}, \bar{J} = J\begin{bmatrix} 0 & 1 & 0 \\ -1 & 0 & 0 \\ 0 & 0 & 0 \end{bmatrix}$$

$$\begin{aligned} f_3 = & -[0 \quad \sin\phi/\cos\theta \quad \cos\phi/\cos\theta] J^{-1}(\omega^b \times J\omega^b) + \\ & q\dot{\phi}\cos\phi/\cos\theta + q\dot{\theta}\sin\theta\sin\phi/\cos^2\theta - \\ & r\dot{\phi}\sin\phi/\cos\theta + r\dot{\theta}\sin\theta\cos\phi/\cos^2\theta \end{aligned}$$

$$g_3 = [0 \quad \sin\phi/\cos\theta \quad \cos\phi/\cos\theta] J^{-1},$$

$$u = [(\tau^b)^T \quad \ddot{Z}]^T$$

The disturbances of Δ_1 and $h_2\Delta_1$ can be measured by linear accelerometers, but we can not obtain the disturbance ζ since the angular acceleration is difficult to measure (He & Han, 2007). In this section, we use the estimated disturbances ζ in section 5.3 into the acceleration feedback control (AFC) scheme, proposed in He and Han's paper (He & Han, 2007) and shown as Fig. 8, to attenuate its influence on the closed loop performance. And the detailed designing processes are as follows,

Step I:

Design a nonlinear H∞ controller with measurable disturbances of (58) based on He's AFC based controller design method by taking $u_1 = g_2(p_1, \dot{p}_1, p_2, \dot{p}_2)u$ as independent inputs.

Step II:

With respect Eq. (59), design the following feedback linearization controller with estimated disturbances of (59) by taking $u_2 = g_3(p_2, \dot{p}_2, \psi, \dot{\psi})u$ as independent inputs.

$$u_2 = -f_3(p_2, \dot{p}_2, \psi, \dot{\psi}) - \hat{\zeta} \tag{60}$$

where k_1 and k_2 are positive constant; $\hat{\zeta}$ is the estimated disturbance and can be obtained by construct a dynamic model as Eq. (55).

Step III:

Obtain the control input u,

$$u = \begin{bmatrix} g_2(p_1, \dot{p}_1, p_2, \dot{p}_2) \\ g_3(p_2, \dot{p}_2, \psi, \dot{\psi}) \end{bmatrix}^{-1} \begin{bmatrix} u_1 \\ u_2 \end{bmatrix} \tag{61}$$

Step IV:

Compute the real inputs as Eq. (49) and Eq. (61). ■

The estimator parameters are the same as Eq. (57). And the following parameters are selected to construct the preceding controller,

$$k_1 = k_2 = 4$$

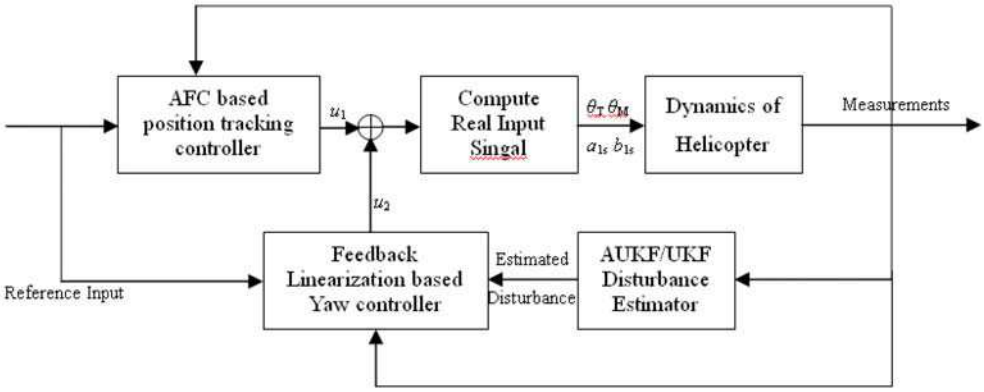

Fig. 8. Tracking Controller Structure of Model Helicopter

Fig. 9 shows the time response of the closed loop. From which, with the AUKF estimator, the yaw angle can go back to the desired value more quickly that that of UKF, and thus, it is clear that the controller with the AUKF has better attenuation disturbance performance.

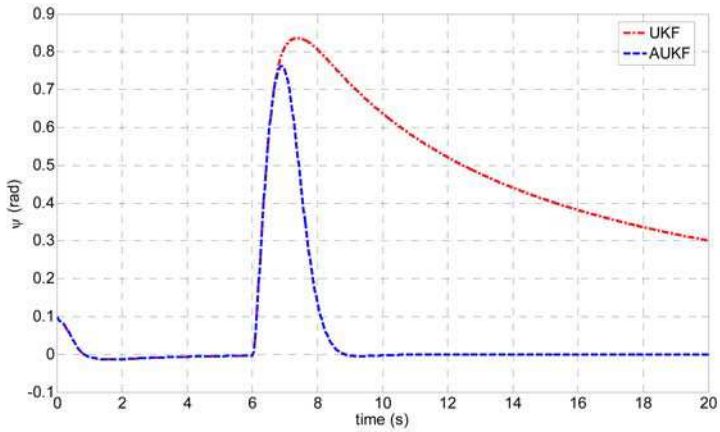

Fig. 9. Time Response of Yaw Angle With Tracking Controller

6. Conclusions

In this Chapter, two adaptive Unscented Kalman Filters (AUKFs), named MIT rule based AUKF and master-slave AUKF, are introduced respectively with the purpose of handling time-varying or uncertain noise distribution. According to the simulation results conducted on omni-directional mobile robot and model helicopter, we can conclude the followings:

1. With incorrect *a priori* statistic information, the AUKFs perform much better than the normal UKF does.
2. Although achieving a little higher estimation precision than the MS-AUKF does, the MITAUK suffers more complicated calculations. That means, the MS-AUKF is appropriate for the application where computation resources are critical. The MS-AUKF, on the other hand, would meet the requirement of high precision estimation.

3. The proposed AUKF is feasible to be integrated into robust control scheme, to effectively reject the uncertainty/disturbance that are difficult for actually measured or off-line modelled.

7. References

Chaer, W. S.; Bishop, R. H. & Ghosh, J. (1997). A mixture-of-experts framework for adaptive Kalman filtering. *IEEE Transactions on Systems, Man and Cybemetics, Part B: Cybemetics*, Vol. 27, No. 3, pp. 452-464

El-Fattah, Y. M. (1983). Recursive self-tuning algorithm for adaptive Kalman filtering. *IEE Proceedings*, Vol. 130, No. 6, pp. 341-344

Garcia-Velo, J. (1997). Determination of noise covariances for extended Kalman filter parameter estimators to account for modeling errors, Ph.D. thesis, University of Cincinnati

He, Y. Q. & Han. J. D. (2007). Acceleration Feedback Enhanced H∞ Disturbance Attenuation Control, *The 33rd Annual Conference of the IEEE Industrial Electronics Society (IECON)*, pp. 839-844, Taipei

Hu, C.; Chen, W.; Chen,Y. & Liu., D. (2003). Adaptive Kalman filtering for vehicle navigation. *Journal of Global Positioning Systems*, Vol. 2, No. 1, pp. 42-47

Jazwinski, A. H. (1970). "Stochastic processes and filtering theory," Academic Press, New York, 1970.

Julier, S. J.; Uhlmann, J. K. & Durrant-Whyte, H. F. (1995). A new approach for filtering nonlinear systems. *Proceedings of the American Control Conference*, pp. 1628-1632, Seattle

Koo, T. & Sastry, S. (1998). Output tracking control design of a helicopter model based on approximated linearization, *Proceedings of the 37th IEEE conference on Decision & Control*, pp. 3625-3640, Tampa

Lee, D. J. & Alfriend, K. T. (2004). Adaptive sigma point filtering for state and parameter estimation. *AIAA/AAS Astrodynamics Specialist Conference and Exhibit*, pp. 1-20, Rhode Island

Ljung, L. (1977). Analysis of recursive stochastic algorithms. *IEEE Transactions on Automatic Control*, Vol. 22, No. 4, pp. 551-575

Loebis, D.; Sutton, R.; Chudley, J.; & Naeem, W. (2004). Adaptive tuning of a Kalman filter via fuzzy logic for an intelligent AUV navigation system, *Control Engineering Practice*, Vol. 12, No. 12, pp. 1531-1539

Maybeck, P. S. (1979). *Stochastic Models, Estimation and Control.* New York: Academic Press

Mehra, R. K. (1970). On the identification of variances and adaptive Kalman filtering. *IEEE Transactions on Automatic Control*, Vol. 15, No. 2, pp. 175-184

Mohamed, A. H. & Schwarz, K. P. (1999). Adaptive Kalman filtering for INS/GPS. *Journal of Geodesy*, Vol. 73, No. 4, pp. 193-203

Napolitano, M.; An, Y. & Seanor, B. (2000). A Fault Tolerance Flight Control System for Sensor and Actuator Failures Using Neural Networks. *Aircraft Design*, 2000, 3(2): 103-128.

Noriega,G. & Pasupathy, S. (1997). Adaptive Estimation of Noise Covariance Matrices in Real-Time Preprocessing of Geophysical Data. *IEEE Transactions on Geoscience and Remote Sensing*, Vol. 35, No. 5, pp. 1146-1159

Pesonen, U.; Steck, J & Rokhsaz K. (2004). Adaptive neural network inverse controller for general aviation safety. *Journal of Guidance, Control, and Dynamics*, 2004, 27(3): 434-443

Shim, D. H. (2000). Hierarchical flight control system synthesis for rotorcraft-based unmanned aerial vehicles. Ph.D. thesis, University of California

Song, Q. & Han, J. D. (2007). A novel adaptive unscented Kalman filter for nonlinear estimation. Proceedings of the 46th IEEE Conference on Decision and Control, pp. 4293-4298. New Orleans

Song, Y. X. (2002). *Study on trajectory tracking control of mobile robot with orthogonal wheeled assemblies.* Ph.D. thesis, Shenyang Institute of Automation, Chinese Academy of Sciences

Van der Merwe, R. &Wan, E. A. (2001). The squre-root unscented Kalman filter for state and paramter estimation, *Proceedings of the IEEE International Conference on Acoustics, Speech, and Signal Processing*, pp. 3461-3464. Soat Late City

Wan, E. A. & Van der Merwe, R. (2000). The unscented Kalman filter for nonlinear estimation. *Proceeding of the Symposium 2000 on Adaptive System for Signal Processing, Communication and Control (AS-SPCC)*, pp. 153-158. Lake Louise

Kalman Filter Recent Advances and Applications

Edited by Victor M. Moreno and Alberto Pigazo

ISBN 978-953-307-000-1
Hard cover, 584 pages
Publisher InTech
Published online 01, April, 2009
Published in print edition April, 2009

The aim of this book is to provide an overview of recent developments in Kalman filter theory and their applications in engineering and scientific fields. The book is divided into 24 chapters and organized in five blocks corresponding to recent advances in Kalman filtering theory, applications in medical and biological sciences, tracking and positioning systems, electrical engineering and, finally, industrial processes and communication networks.

How to reference

In order to correctly reference this scholarly work, feel free to copy and paste the following:

Jianda Han, Qi Song and Yuqing He (2009). Adaptive Unscented Kalman Filter and Its Applications in Nonlinear Control, Kalman Filter Recent Advances and Applications, Victor M. Moreno and Alberto Pigazo (Ed.), ISBN: 978-953-307-000-1, InTech, Available from: http://www.intechopen.com/books/kalman_filter_recent_adavnces_and_applications/adaptive_unscented_kalman_filter_and_its_applications_in_nonlinear_control

INTECH
open science | open minds

InTech Europe
University Campus STeP Ri
Slavka Krautzeka 83/A
51000 Rijeka, Croatia
Phone: +385 (51) 770 447
Fax: +385 (51) 686 166
www.intechopen.com

InTech China
Unit 405, Office Block, Hotel Equatorial Shanghai
No.65, Yan An Road (West), Shanghai, 200040, China
中国上海市延安西路65号上海国际贵都大饭店办公楼405单元
Phone: +86-21-62489820
Fax: +86-21-62489821